



# Physical and biological property comparisons of $^4\text{He}$ and $^3\text{He}$ ion beams for applicability in radiation therapy

**Kristaps Paļskis (RTU, CERN)**

*Under the supervision of*      *prof. Toms Torims (RTU)*

*Maurizio Vretenar (CERN)*

*prof. Joao Seco (DKFZ)*

*Mariusz Sapinski (PSI, SEEIIST)*

## Background:

# Helium ions for particle therapy

- Proving intermediate physical and biological characteristics between protons and carbon ions, **helium ion therapy is returning to «novelty horizon»**
- Clinically – helium-4 ion beams are mainly considered

**There is another stable helium isotope to consider for ion therapy: Helium-3**

# Background: In favour of helium-3

Helium-3 ions provide favourable characteristics from accelerator physics point-of-view due to their charge-to-mass ratio of  $2/3$  compared to  $1/2$  of  $^4\text{He}$ :

## Beam rigidity

For the same maximum range of 30 cm in water:

for  $^3\text{He}$ : 260 MeV/u

for  $^4\text{He}$ : 220 MeV/u

Corresponding magnetic rigidity:

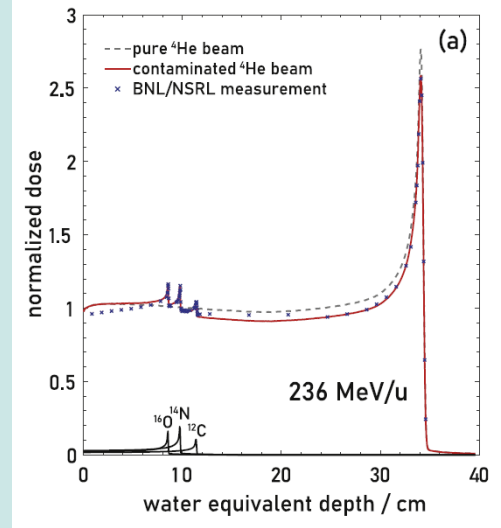
for  $^3\text{He}$ : 3.74 T\*m

for  $^4\text{He}$ : 4.52 T\*m

Same magnetic field –  
1.2 lower ring radius

## Contamination at injection

For  $^4\text{He}$ , other ion species with  $q/m = 1/2$  from the plasma source can contaminate the beam at injection  
( $^{12}\text{C}$ ,  $^{14}\text{N}$ ,  $^{16}\text{O}$ )





# Background:

## Clinically relevant physics of $^3\text{He}$

With the rationale from favourable accelerator performance with the use of  $^3\text{He}$  beams, question is

**How do  $^3\text{He}$  ion beam differs from  $^4\text{He}$  ion beam parameters in relevant physical and biological aspects for a clinical use?**

# The aim of this work

Linear Energy  
Transfer  
distributions

Physical dose:  
Depth dose and lateral  
profiles

Neutron fluence  
and kinetic energy  
distributions

Within a simulation framework,  
compare  $^3\text{He}$  and  $^4\text{He}$  ion  
beams, extracting relevant  
physical and biological  
parameters for clinical use

Biological dose:  
RBE distributions

# The aim of this work

Linear Energy  
Transfer  
distributions

Physical dose:  
Depth dose and lateral  
profiles

Neutron fluence  
and kinetic energy  
distributions

Within a simulation framework,  
compare  $^3\text{He}$  and  $^4\text{He}$  ion  
beams, extracting relevant  
physical and biological  
parameters for clinical use

Positron emitter  
distributions

Biological dose:  
RBE distributions

Prompt gamma  
emissions

## Main simulation parameters

- Geant4 simulation framework for **unperturbed beams**  
(*no initial energy spread and contamination*)
  - $10^6$  particles in **water** – dose distribution parameter estimation
  - $10^7$  particles in **skeletal muscle tissue** – positron emitter and prompt gamma yield estimation
- Initial energies for range of 100–150 mm in water
  - **129.8 to 180.1 MeV/u for  $^3\text{He}$**
  - **109.3 to 151.3 MeV/u for  $^4\text{He}$**
- Physical quantities scored:
  - Energy deposition and LET by particle type
  - Kinetic energy by particle type
  - Neutron fluence and kinetic energy
  - Positron emitter isotope yields and spatial distributions
  - Vertex data of prompt gamma emissions + corresponding process and parent particles

## Main calculational aspects

### Physical dose distribution calculations

Physical dose based spread-out Bragg peak optimization  
( *superposition of pristine Bragg peaks* )

### Relative Biological Effectiveness calculations, biologically driven optimization

Relative Biological Effectiveness calculation with Microdosimetric Kinetic model  
Biologically driven spread-out Bragg peak optimization

### Positron emitters signal estimation

Yield distribution conversion into integrated activity  
Positron range considerations for activity distribution

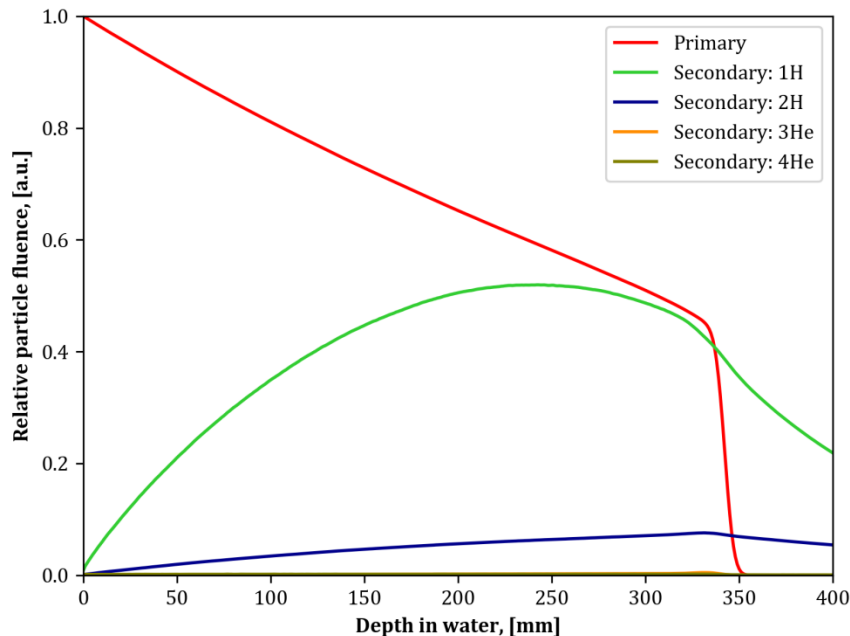
### Prompt gamma signal estimation

Prompt gamma energy spectrum and emission depth distribution  
Prompt gamma spectrum separation by physical interaction processes

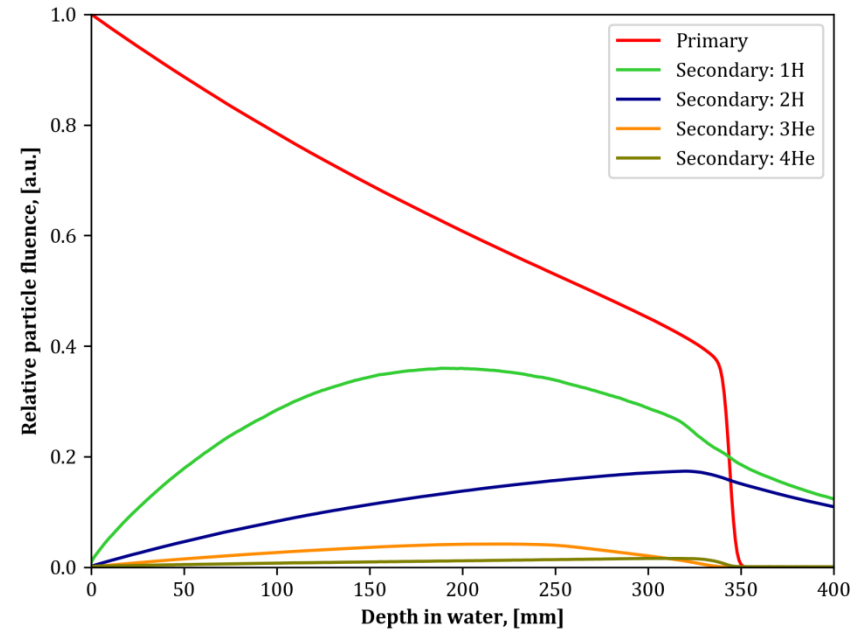


## Constituents of the *mixed beam*

Undergoing matter interactions, particle beam is *mixed* – primary helium ions and various secondaries  
(*projectile fragmentation and target fragmentation*)

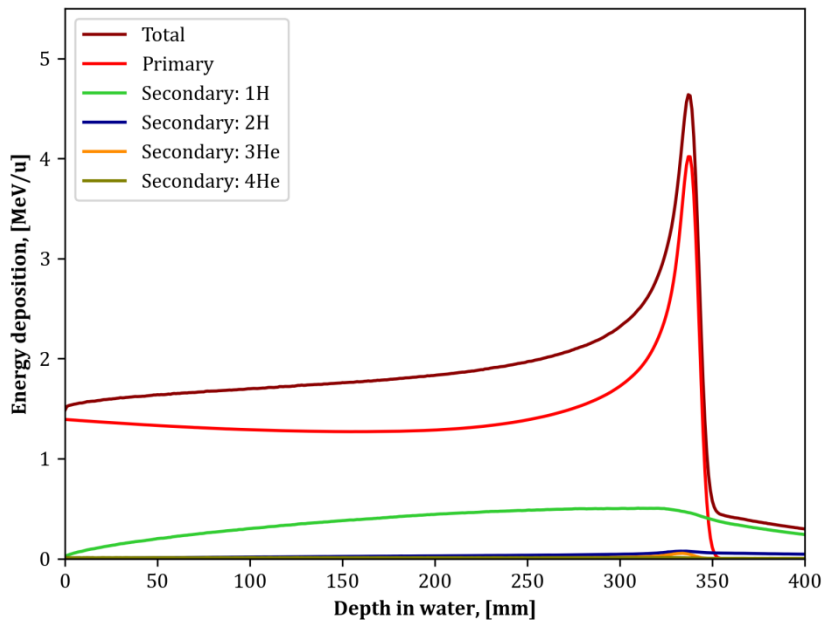


Particle fluences of main constituents of  $^3\text{He}$  beam  
( $r = 35\text{cm}$ ,  $E = 278.2\text{ MeV/u}$ )



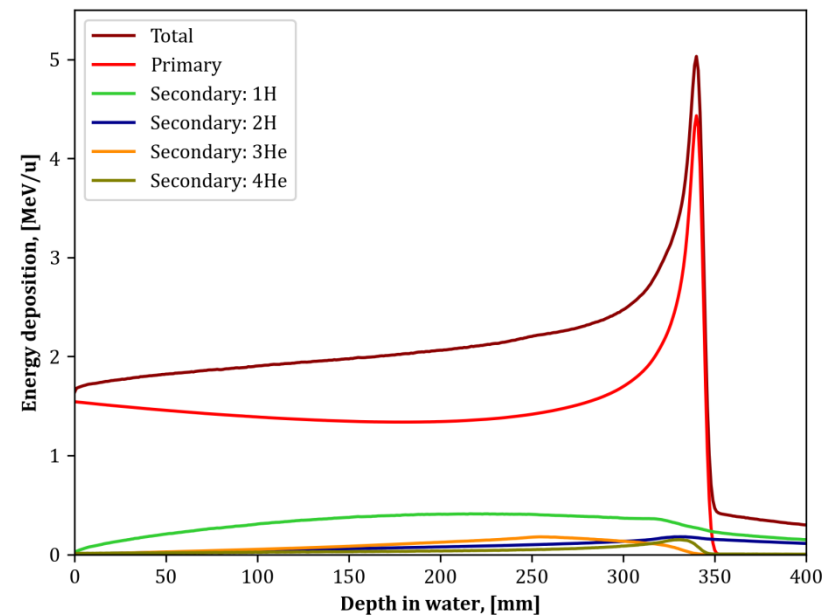
Particle fluences of main constituents of  $^4\text{He}$  beam  
( $r = 35\text{cm}$ ,  $E = 234\text{ MeV/u}$ )

## Constituents of the *mixed beam*



Energy deposition of main constituents of  $^3\text{He}$  beam

( $r = 35\text{cm}$ ,  $E = 278.2\text{ MeV/u}$ )



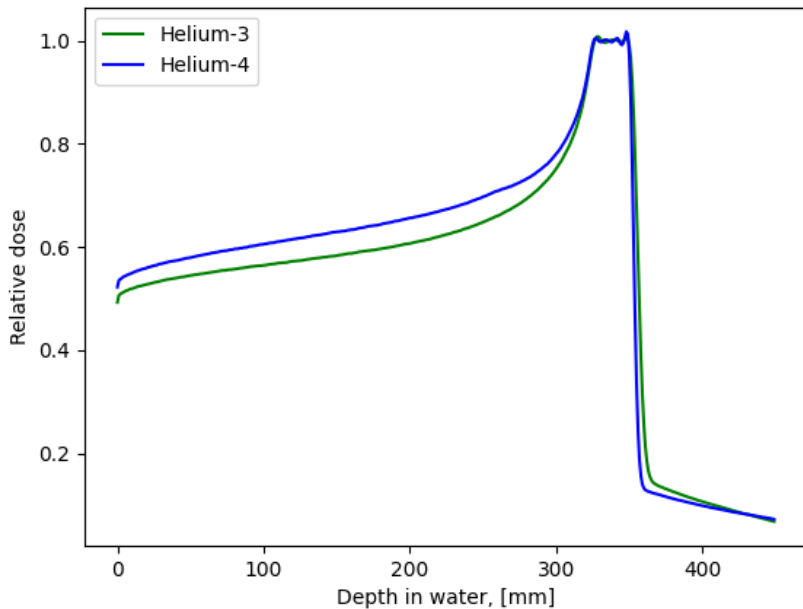
Energy deposition of main constituents of  $^4\text{He}$  beam

( $r = 35\text{cm}$ ,  $E = 234\text{ MeV/u}$ )

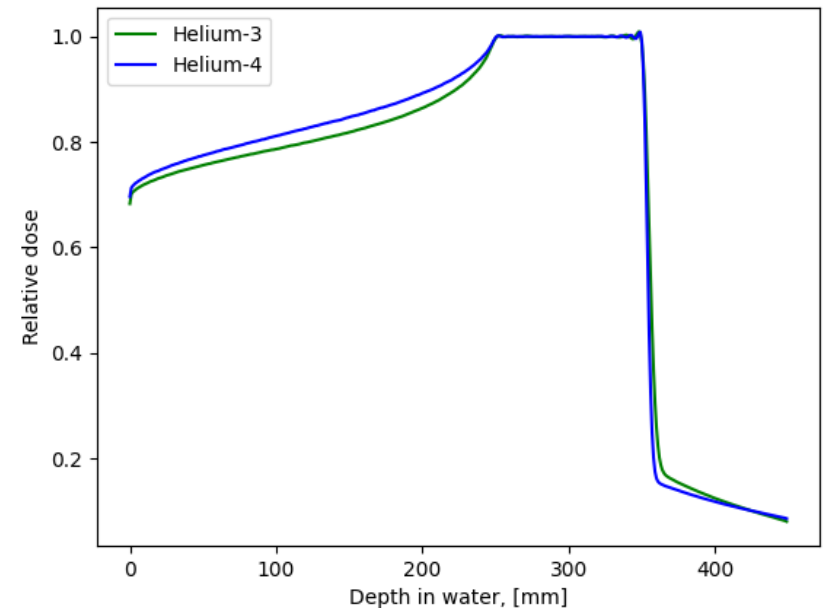
$^4\text{He}$  ion beams *undergo* more nuclear reactions, resulting in steeper decrease of primary fluence and higher contributions of secondary fragments

## Physical SOBPs: IDD approach

*IDD – integrated depth dose, radially integrated all deposition contributions*



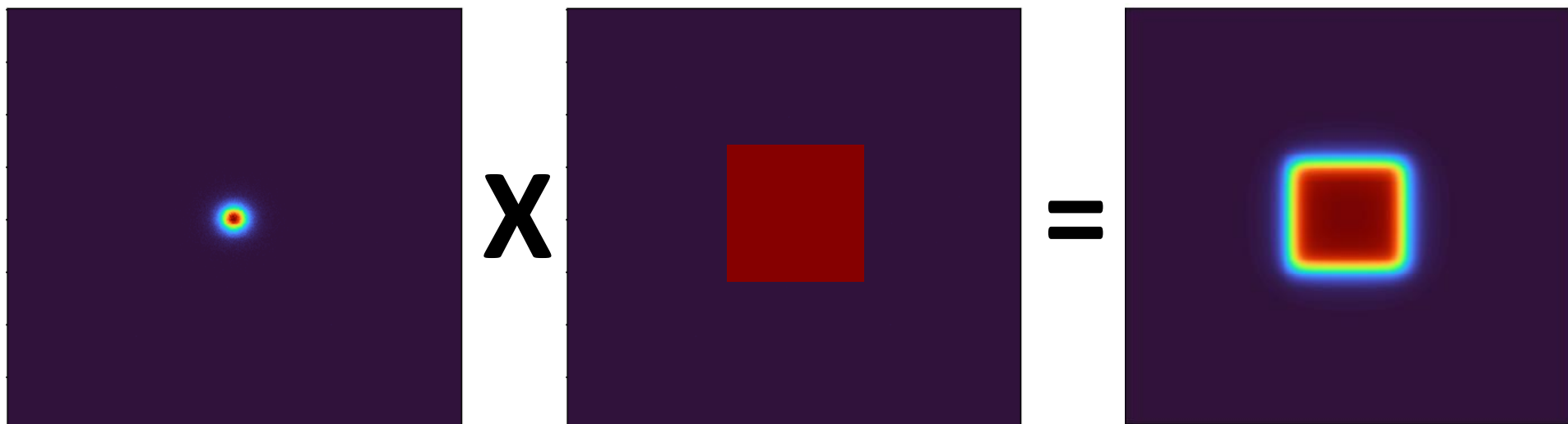
Physically optimized SOBP:  
25 mm length, distal end at 350 mm



Physically optimized SOBP:  
100 mm length, distal end at 350 mm

**<sup>3</sup>He beams – lower entrance dose ( up to 5%)**  
*exhibits more at large depths and smaller tumors*

## Physical SOBPs: PB convolution



Energy deposition  
pencil beam  
(kernel)

Fluence map  
(*radiation field*)

Dose distribution  
corresponding to a  
particular radiation  
field

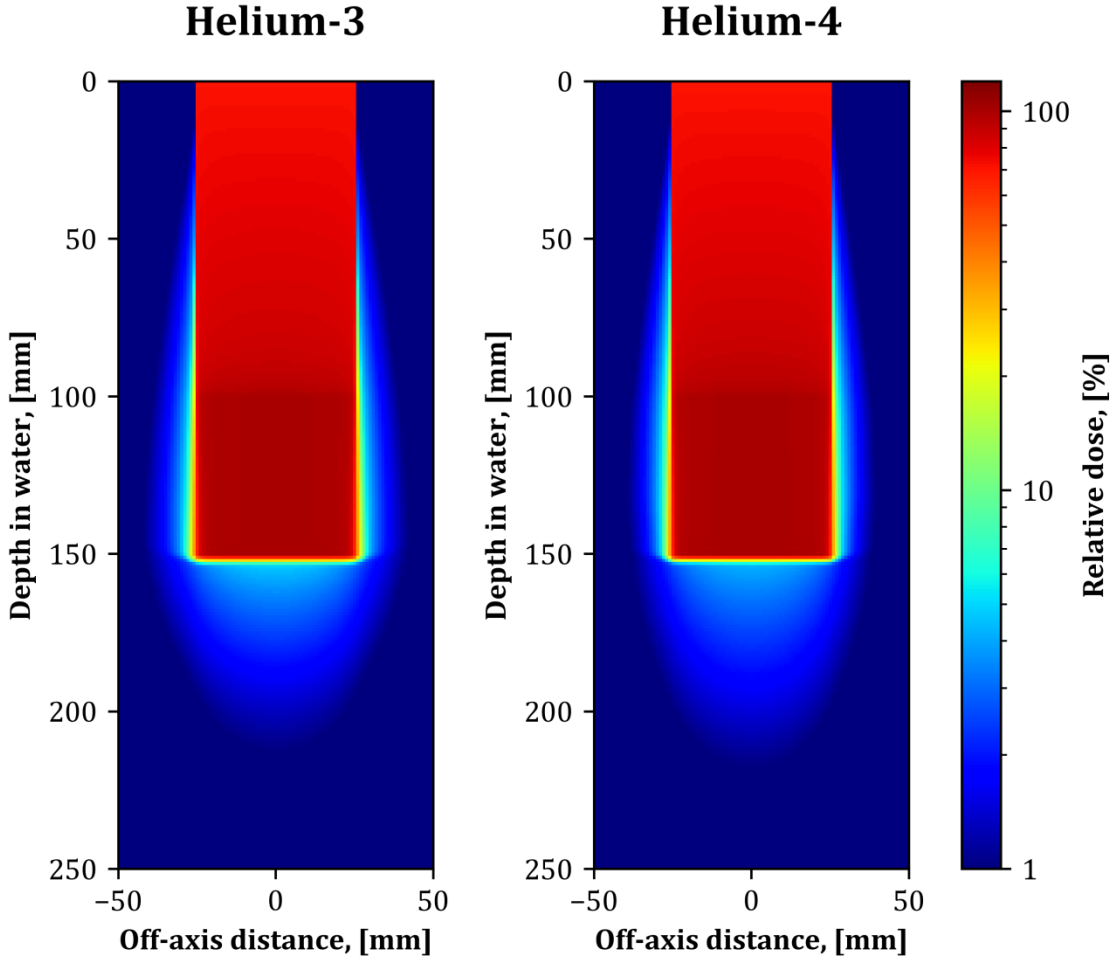


# Results

## Physical SOBPs: 2.5D distribution

Dose distribution map for a simulated 5x5x5 tumor at 15 cm distal depth  
( left -  $^3\text{He}$  ions, right -  $^4\text{He}$  ions )

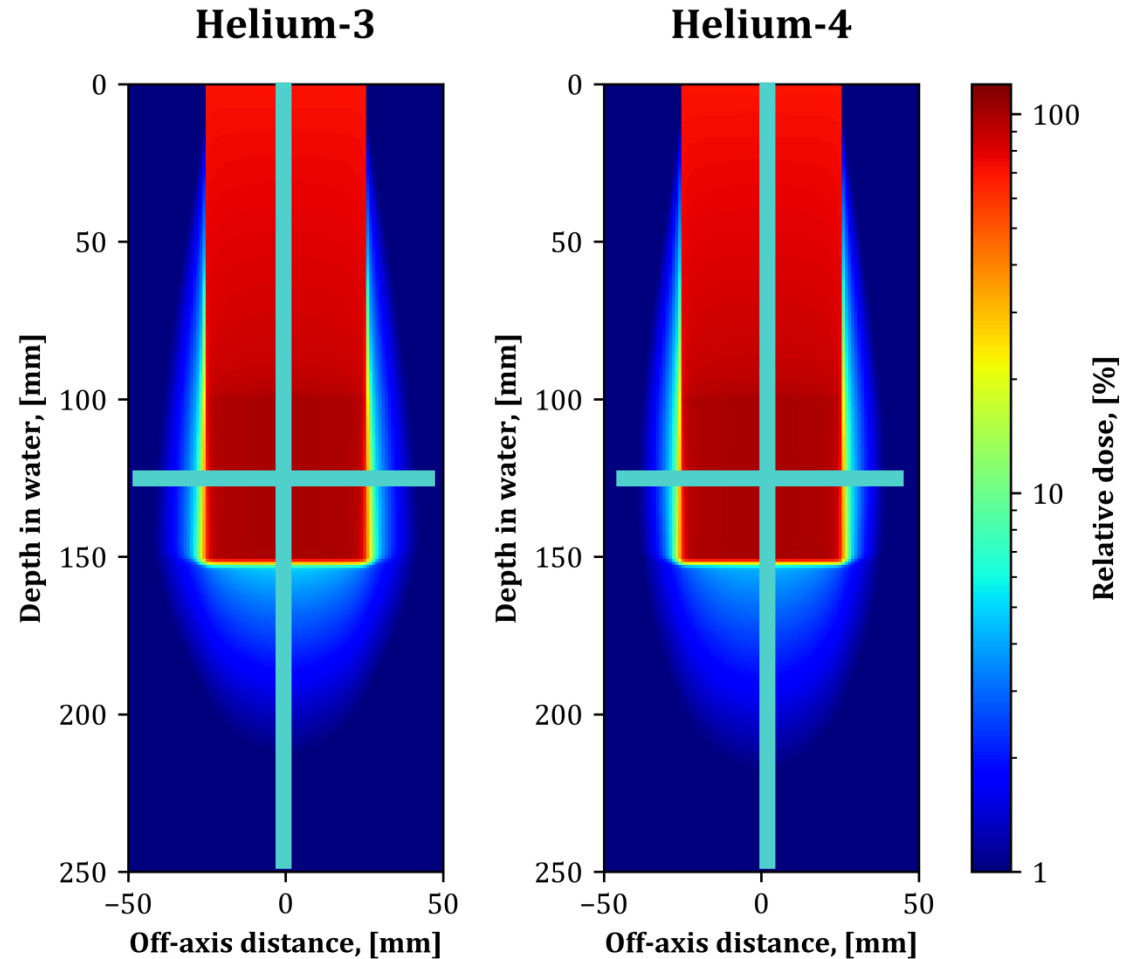
**$^3\text{He}$  beams exhibit broader lateral distribution due to scattering.  
Fragmentation tail narrower, more «forward-peaked» for  $^4\text{He}$  ion beams**



## Physical SOBPs: 2.5D distribution

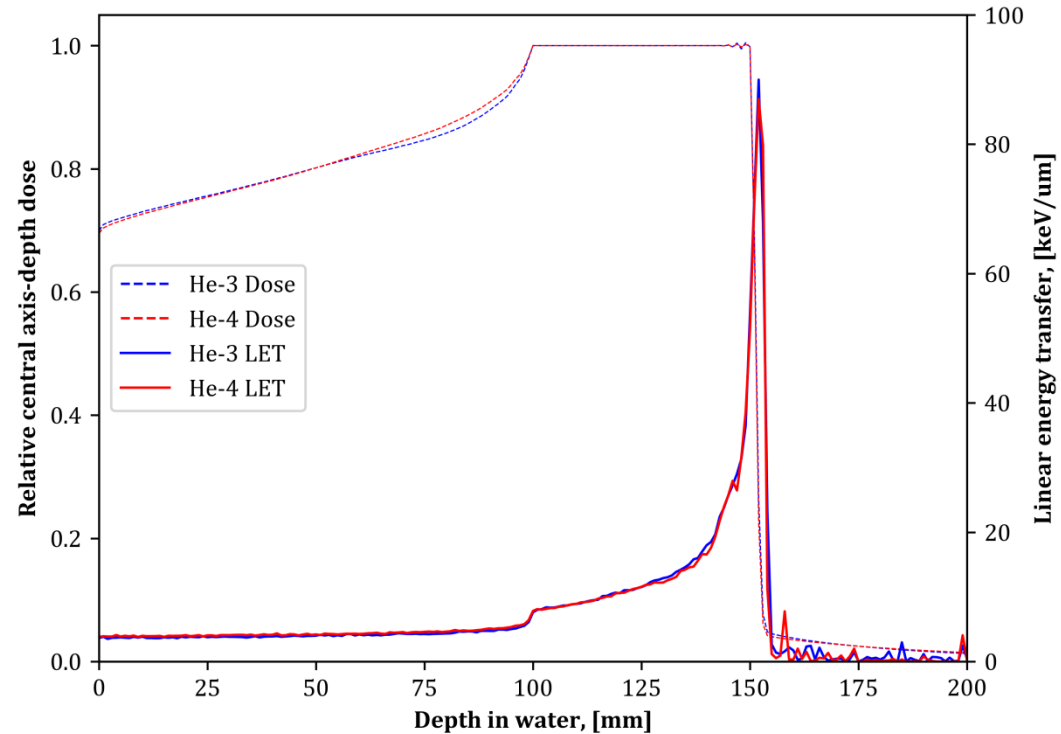
Dose distribution map for a simulated 5x5x5 tumor at 15 cm distal depth  
( left -  $^3\text{He}$  ions, right -  $^4\text{He}$  ions )

$^3\text{He}$  beams exhibit broader lateral distribution due to scattering.  
Fragmentation tail narrower, more «forward-peaked» for  $^4\text{He}$  ion beams



## Central axis depth dose and LET

Central axis depth dose and corresponding LET distribution



Central axis depth distribution and corresponding LET distribution comparison for a simulated 5x5x5 tumor irradiation

**$^3\text{He}$  beams exhibit lower central axis entrance dose**

**Linear energy transfer values are comparable, BUT heavily affected by initial beam conditions (realistic beam) (typically - higher for  $^4\text{He}$ )**



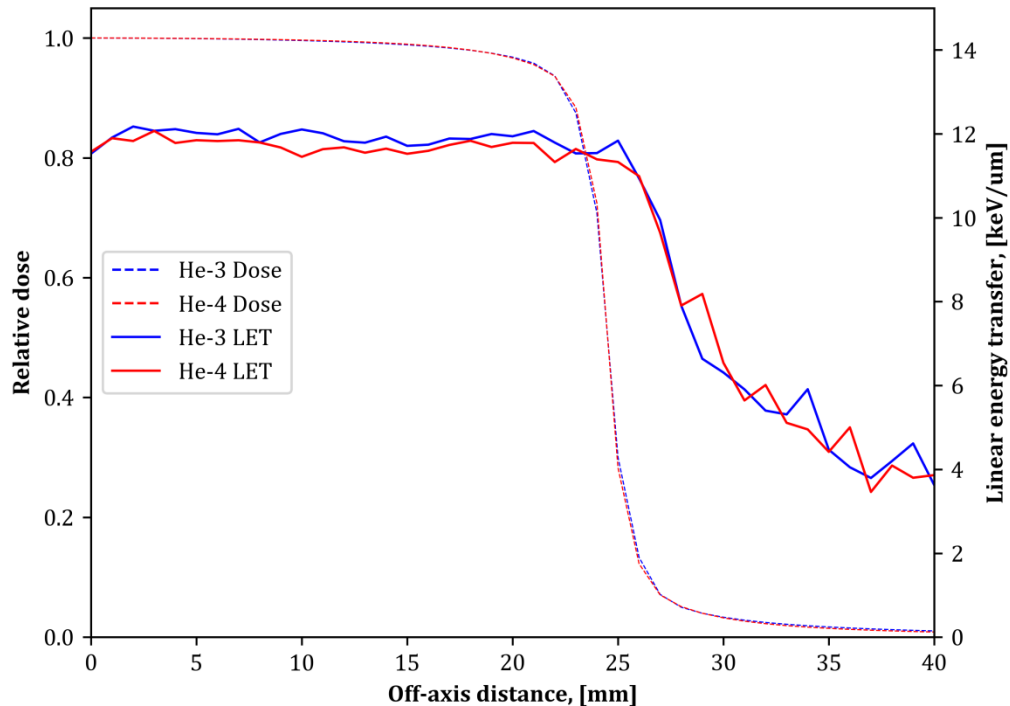
# Results

## Lateral profiles and LET

Lateral dose profile and corresponding LET distribution d=125 mm

**<sup>4</sup>He beams exhibit *sharper* dose profile, comparing penumbras (80%-20% dose level) calculated at 125mm depth:  
for <sup>3</sup>He beam: 2.7 mm  
for <sup>4</sup>He beam: 2.4 mm**

**Linear energy transfer values are comparable,**



Lateral dose profile and corresponding LET distribution comparison for a simulated 5x5x5 tumor irradiation

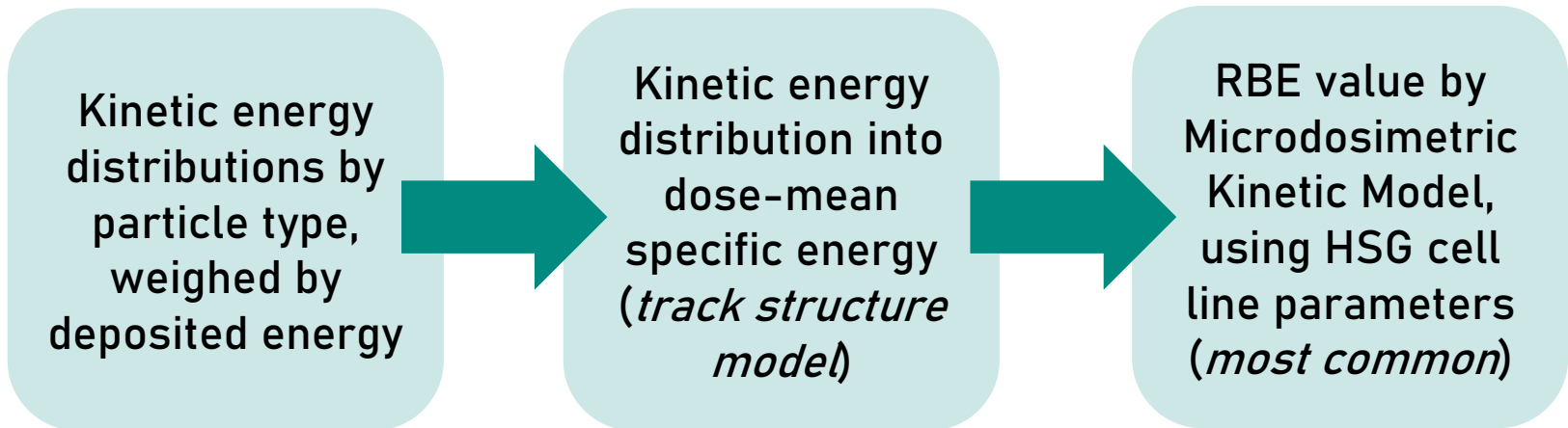




# Results

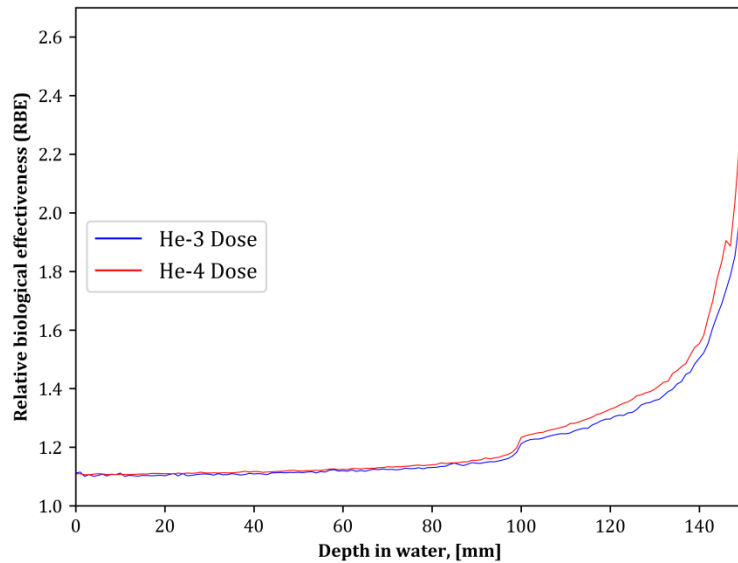
## Relative biological effectiveness

RBE – ratio of physical dose levels needed to deliver same cellular survival level for a particular radiation type compared to reference radiation (conventional gamma photons)



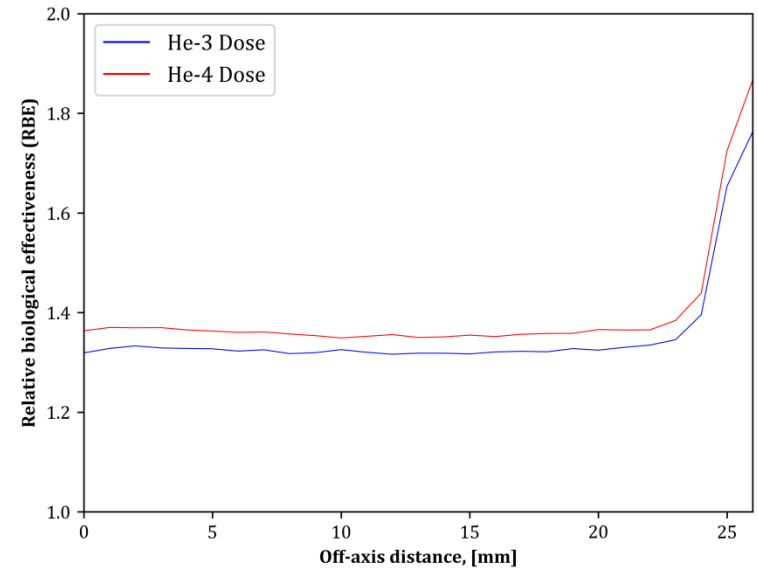
## Relative biological effectiveness

Central axis RBE distribution



Central axis RBE distribution for a simulated 5x5x5 tumor irradiation

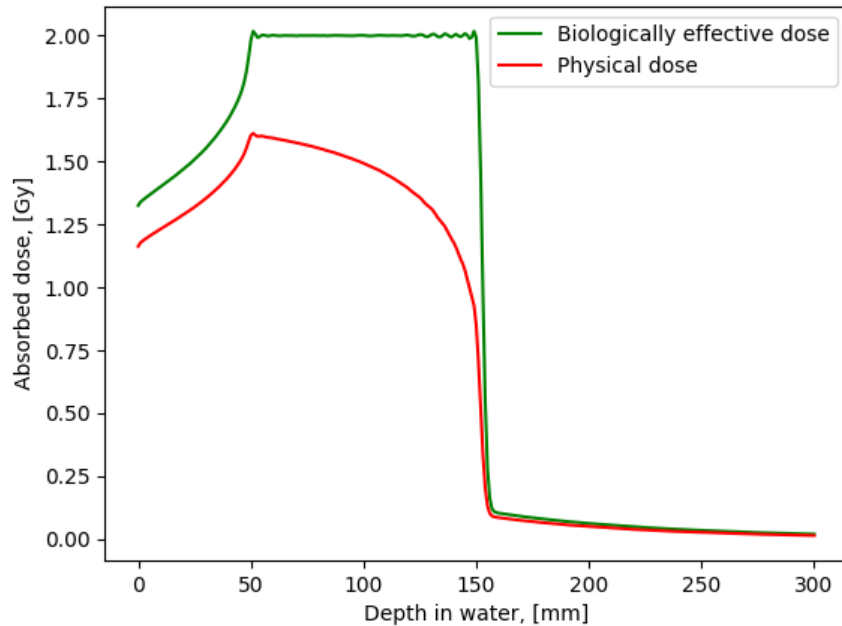
Lateral RBE distribution at depth of 125 mm



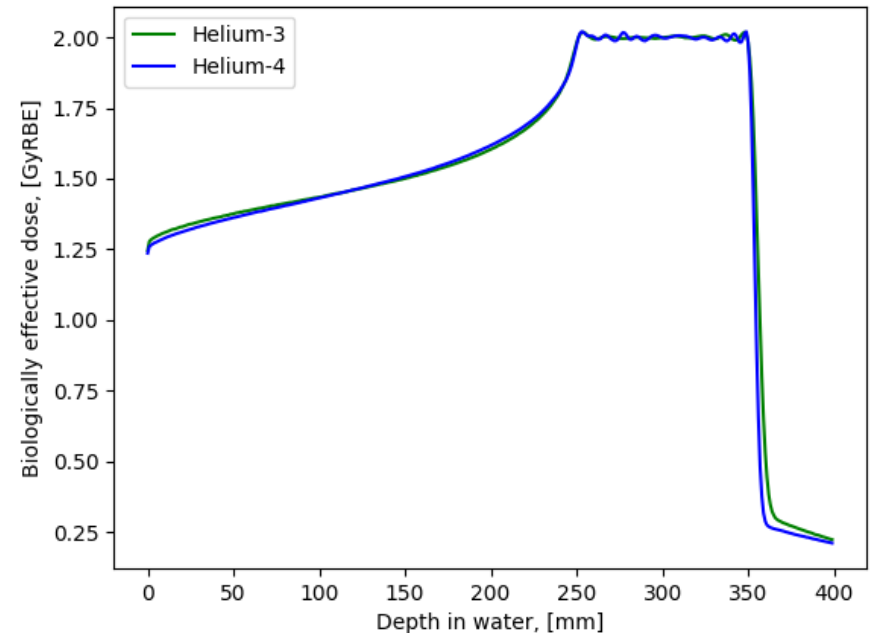
Lateral profile RBE distribution at 125 mm for a simulated 5x5x5 tumor irradiation

**$^4\text{He}$  beams exhibit comparable RBE in entrance channel, while ~ 5% larger RBE in SOBP region**

## Biologically driven optimization



Biologically optimized SOBP: physical and biologically effective dose distributions



Biologically optimized SOBP comparison for  $^3\text{He}$  and  $^4\text{He}$  beams

**Biologically optimized dose distributions show negligible level of differences**

# Treatment range verification

## Ions – main advantage

Ions *stop*, delivering a Bragg peak

## Ions – main challenge

Ions *stop... where is the Bragg peak?*

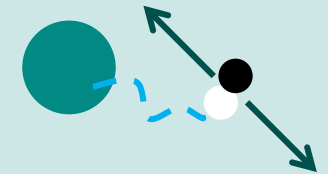
*A priori* – dual energy CT, ion radiography

*On-line* – range verification

## Two main methods

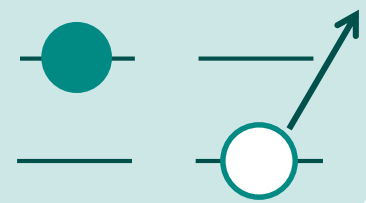
### POSITRON EMITTERS

Nuclear reactions resulting in positron emitting nuclei, registration of the annihilation gammas (PET)

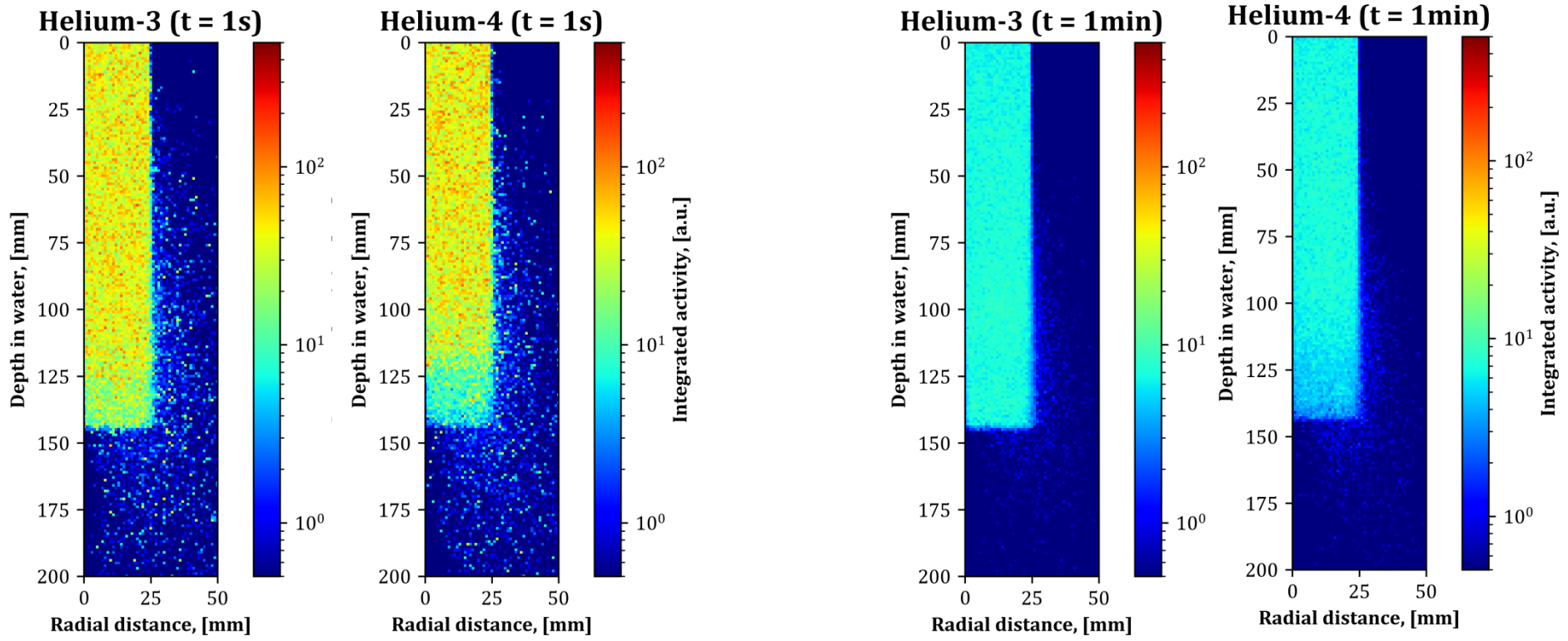


### PROMPT GAMMAS

Nuclear reactions resulting in nuclei in excited states that relax by gamma emissions in ps range



## Positron emitter distributions



Integrated over 1 second

Integrated over 1 minute



# Results

## Positron emitter distributions

$^3\text{He}$  ion beams exhibit 5 – 10 % higher positron emitter production yields per incident particle

$^3\text{He}$  ion beams exhibit lesser signal fall-off at distal end of the Bragg peak, owing to better correlation with dose distribution – **important factor for range verification**

### Main signal components Long lived

Positron emitter	$T_{1/2}$
$^{15}\text{O}$	122 s
$^{13}\text{N}$	9.97 min
$^{11}\text{C}$	20.34 min

### Main signal components Short lived

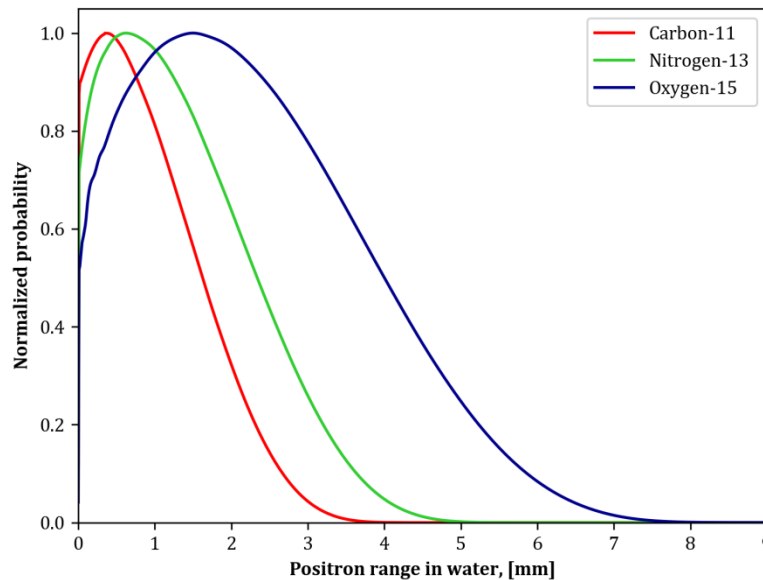
Positron emitter	$T_{1/2}$
$^{12}\text{N}$	11 ms
$^8\text{B}$	772 ms

## «To do»: ADF introduction

Radioactivity map –  
emission of positrons  
Positrons have range in a  
material

ADF

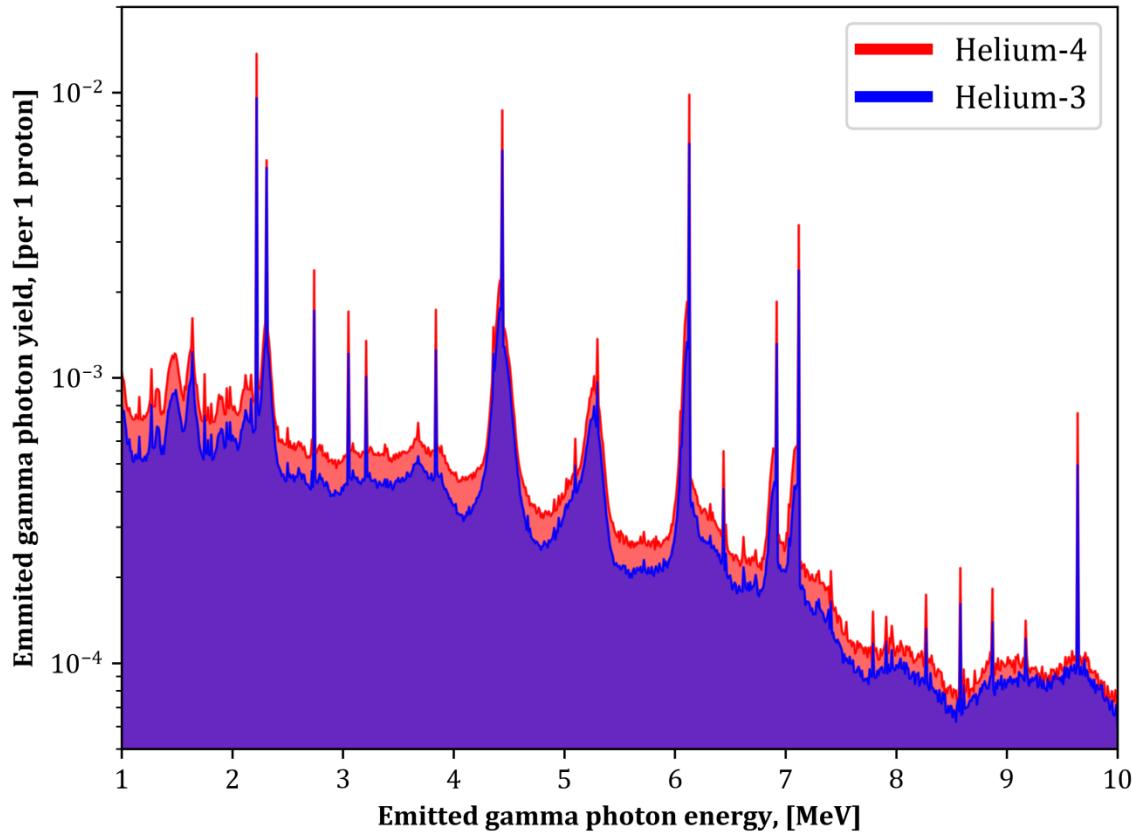
Positron annihilation  
vertexes – Signal obtainable  
by PET



Convolution kernels to use  
with radioactivity map –  
obtainable annihilation  
signal

## Prompt gamma emission spectrum

Spectra of emitted prompt gamma photons



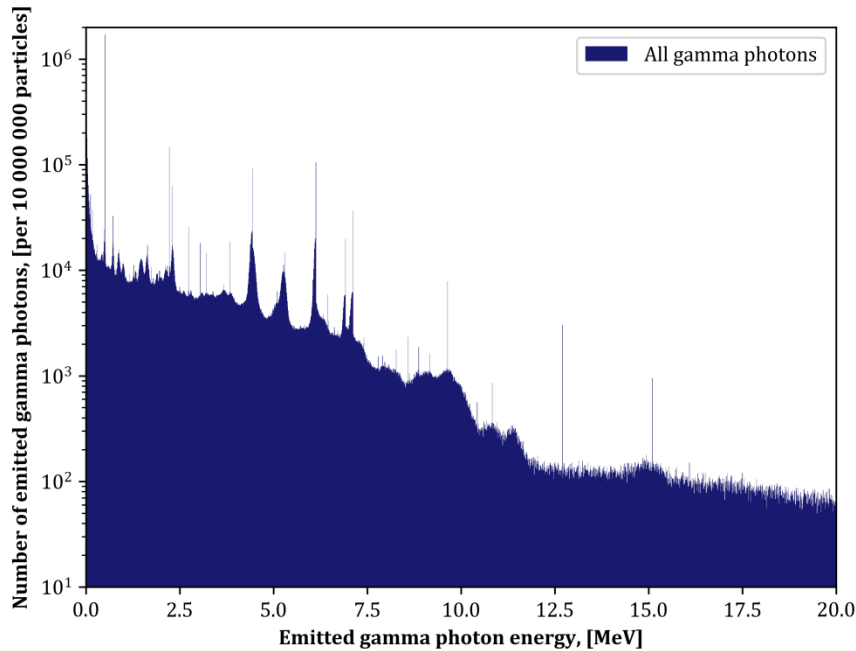
Prompt gamma emission spectrum for pristine Bragg peaks of  $^3\text{He}$  and  $^4\text{He}$  ion beams corresponding to 15 cm range

$^4\text{He}$  ion beams exhibit higher production yields of prompt gammas – around 1.2 – 1.3 times higher

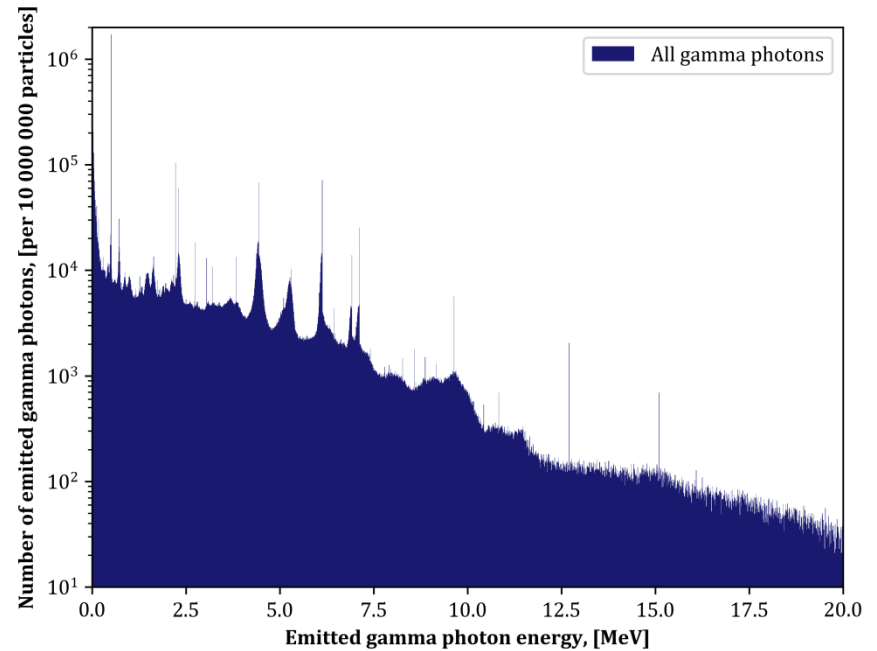


# Results

## Spectrum components



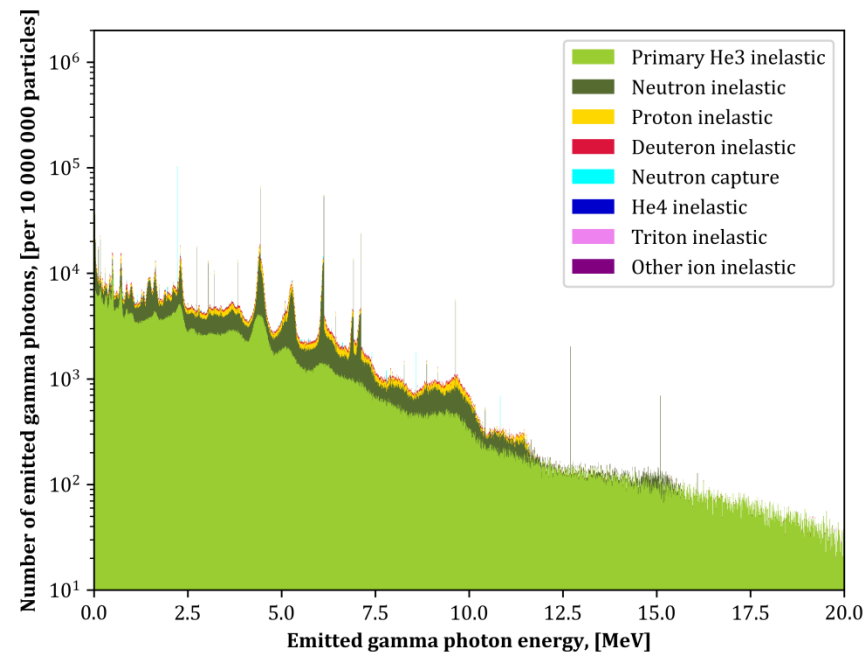
$^3\text{He}$  ion beam prompt  
gamma emission spectrum



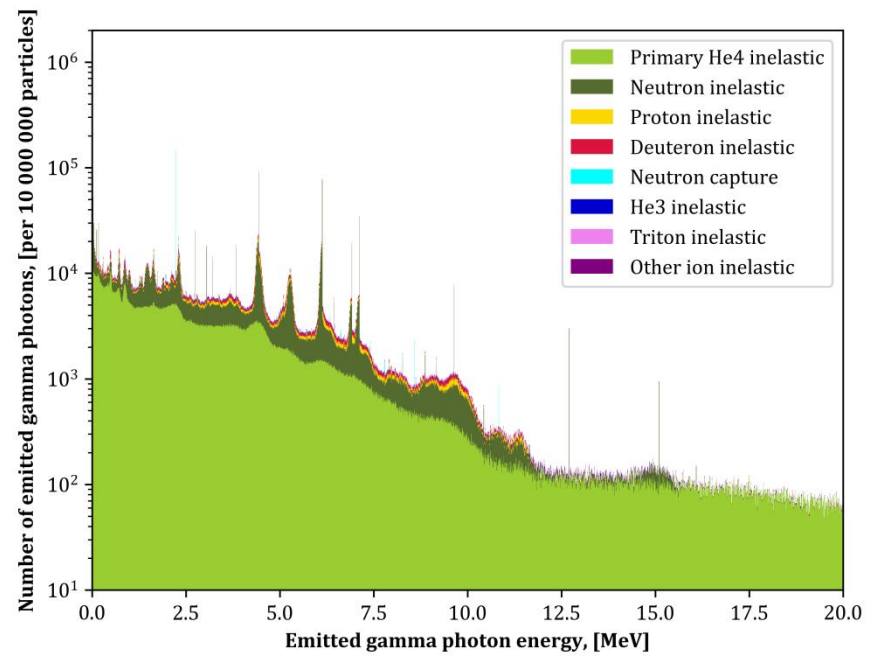
$^4\text{He}$  ion beam prompt  
gamma emission spectrum

# Results

## Spectrum components



$^3\text{He}$  ion beam prompt gamma emission spectrum

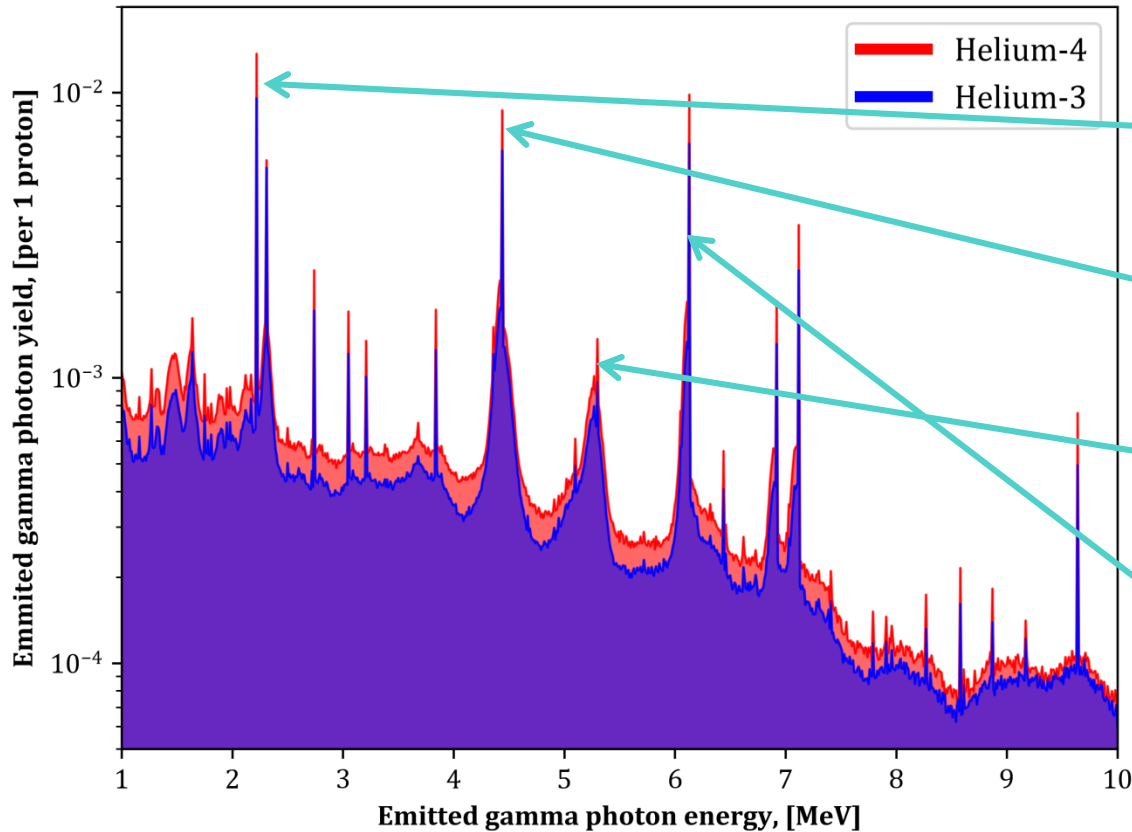


$^4\text{He}$  ion beam prompt gamma emission spectrum

# Results

## Emission depth distributions

Spectra of emitted prompt gamma photons



**2.22 MeV:** Neutron capture by hydrogen

**4.44 MeV:** De-excitation of  $^{12}\text{C}$

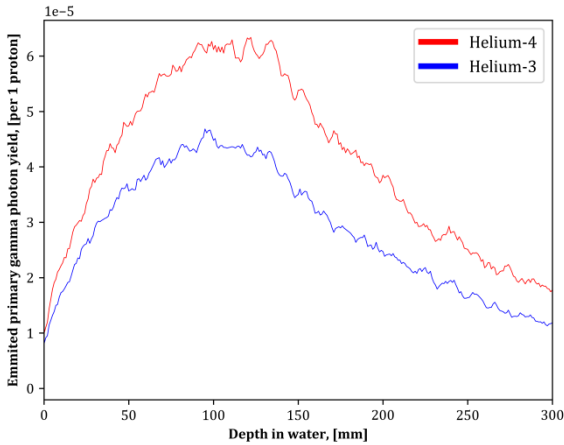
**5.21 MeV:** De-excitation of  $^{15}\text{O}$

**6.13 MeV:** De-excitation of  $^{16}\text{O}$

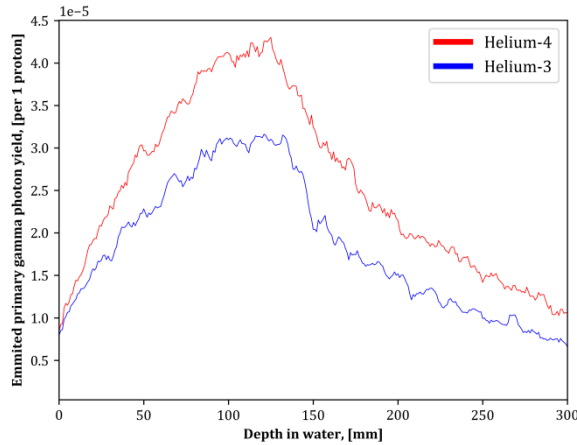
# Results

## Emission depth distributions

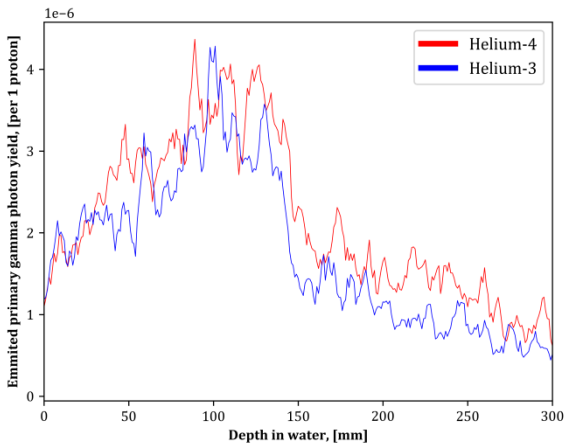
Distribution of emitted primary gamma photons: E=2.22 MeV



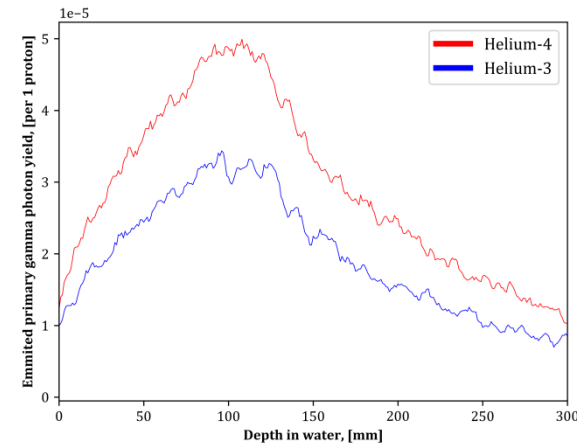
Distribution of emitted primary gamma photons: E=4.44 MeV



Distribution of emitted primary gamma photons: E=5.21 MeV



Distribution of emitted primary gamma photons: E=6.13 MeV



Based on PG emission depth distributions, PG detection at 4.44 or 6.13 MeV would be favourable due to higher signal and sharper fall-off

# Conclusions

- $^4\text{He}$  ion beams exhibit more favourable clinical characteristics in terms of RBE and lateral dose distribution due to scattering
- $^3\text{He}$  ion beams provide favourable physical dose distributions with decreased entrance dose, though this becomes negligible if biological optimization of dose distribution is performed
- In terms of applicability for range verification,  $^3\text{He}$  ion beams provide higher signal level for PET methodology, while  $^4\text{He}$  ion beams – for prompt gamma detection. Though experimental validation of this aspect would be required.

# Conclusions

From accelerator physics point-of-view, the gain of creating smaller sized, more compact synchrotron ring for  $^3\text{He}$  ion beams could be justified with the medical physics findings of this study.



RĪGAS TEHNISKĀ  
UNIVERSITĀTE

**Thank you for your attention!**